Comparative morphology and morphometric assessment of the Neandertal occipital remains from the El Sidrón site (Asturias, Spain: years 2000–2008)

Markus Bastir [a,*], Antonio Rosas [a], Antonio García Tabernero [a], Angel Peña-Melián [b], Almudena Estalrrich [a], Marco de la Rasilla [c], Javier Fortea [c]

[a] PaleoAnthropology Group, Department of Paleobiology, Museo Nacional de Ciencias Naturales (CSIC), C/José Gutiérrez Abascal 2, 28006 Madrid, Spain
[b] Departamento de Anatomía y Embriología Humana I, Facultad de Medicina, Universidad Complutense, Madrid, Spain
[c] Departamento de Historia, Universidad de Oviedo, Calle Teniente Alonso Martínez s/n, Oviedo, Spain

ARTICLE INFO

ABSTRACT

This paper analyses the occipital remains recovered from the El Sidrón (Asturias, Spain) Neandertal site between the years of 2000–2008. The sample is represented by three specimens, SD-1219, SD-1149, and SD-370a. Descriptive morphology, linear measurements, 3D geometric morphometrics, and virtual anthropological methods were employed to address the morphological, morphometric, and phylogenetic affinities of these fossils. The fossils display Neandertal autapomorphies (e.g., bilaterally protruding transverse occipital torus, suprainiac fossa). SD-1219 also preserves a strongly projecting juxtamastoid eminence and shows occipital bunning. In linear distances, the El Sidrón occipitals are similar to each other and close to the Neandertal mean. The centroid size of SD-1219 is slightly larger than the Neandertal average. All of the evidence taken together points to the hypothesis that SD-1219 belongs to a smaller Neandertal male. Linear measurements and the vault thickness of SD-1149 also suggest a robust male individual. The gracility of SD-370a points towards an immature individual. Virtual anthropological methods were used to reconstruct a 3D model of the SD-1219 occipital for geometric morphometrics, which reveals that SD-1219 shows relatively broad and low occipital plane proportions. Within the European Pleistocene lineage sample, this fossil falls geometrically closer to primitive rather than to derived morphologies because of its increased width, and a lower, anterior position of inion relative to the biasterionic axis. These results may imply that cranial sphericity could be an important feature of intraspecific Neandertal variability. Our findings open the way for further studies of intraspecific variation in Neandertal populations, in which the El Sidrón sample may play a significant role.

© 2009 Elsevier Ltd. All rights reserved.

Introduction

A collection of approximately 1600 human fossils has been systematically recovered at the El Sidrón cave site (Asturias, Spain) since 2000, representing the most significant Neandertal sample in the Iberian Peninsula (Rosas and Aguirre, 1999; Fortea et al., 2003; Rosas et al., 2006). The site is located in a small transversal gallery (Galería del Osario) belonging to the El Sidrón karst system (located at the Piloña municipality), and the archaeological material is from a restricted surface not larger than 10 m^2 (Fortea et al., 2003). The human remains have been directly dated to 49 ka by ^{14}C and other methods (Rosas et al., 2006; Torres et al., in press).

The bone assemblage is almost exclusively comprised of human remains belonging to a minimum number of eight individuals (Rosas et al., 2006). All skeletal parts are represented in the sample, including very small bones such as the hyoid and pedal distal phalanges. Among the cranial remains, the most outstanding fossils comprise two frontals, two petrous temporals, and three occipital bones (SD-1219, SD-1149, SD-370a; Figs. 1 and 2), as well as three mandibles (Rosas et al., 2006, 2007). At present, very few macrofaunal remains have been found.

We analyze the El Sidrón occipitals and their place in the European Middle Pleistocene fossil hominin record by means of morphological and morphometric assessment. A detailed analysis of their internal aspect and venous drainage system has been presented elsewhere (Rosas et al., 2008).

Neandertal features on the occipital bone

The occipital bones show several features associated with Neandertals, some of which have been reported as autapomorphies. One autapomorphic trait is a bilaterally protruding transverse
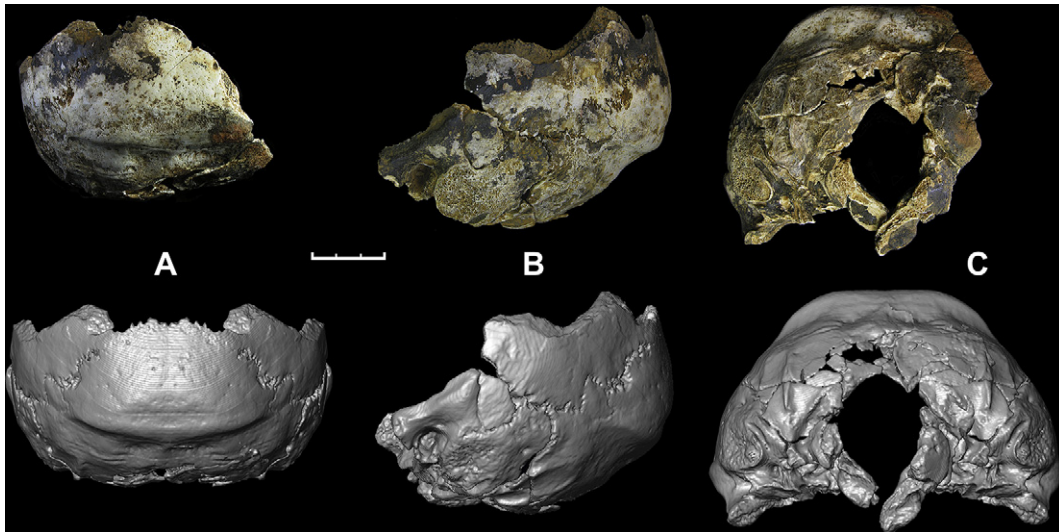
Figure 1. SD-1219. Original fossil (upper part) and virtual reconstruction (lower part). A) posterior, B) left lateral, and C) inferior view of the fossil. Scale bar is 3 cm.

occipital torus with a depression in the midsagittal plane. The upper lip (supreme nuchal line) of the torus delimits the occipital plane superiorly and is very smooth, while the lower lip (superior nuchal line) is more clearly marked and indicates the inferior limit of the occipital plane (e.g., semispinalis muscle fossae) (Hublin, 1978,1984,1998; Arsuaga et al., 1997; Dean et al., 1998).

A second, more disputed Neandertal feature is the suprainiac fossa. While the Neandertal suprainiac fossa is variable in size and shape (Hublin, 1984; Caspari, 2005), it is best defined by a specifically elliptic to oval shaped depression within the transverse occipital torus above inion with a variably porous surface (Hublin, 1978,1984; Arsuaga et al., 1997; Harvati, 2001; Caspari,
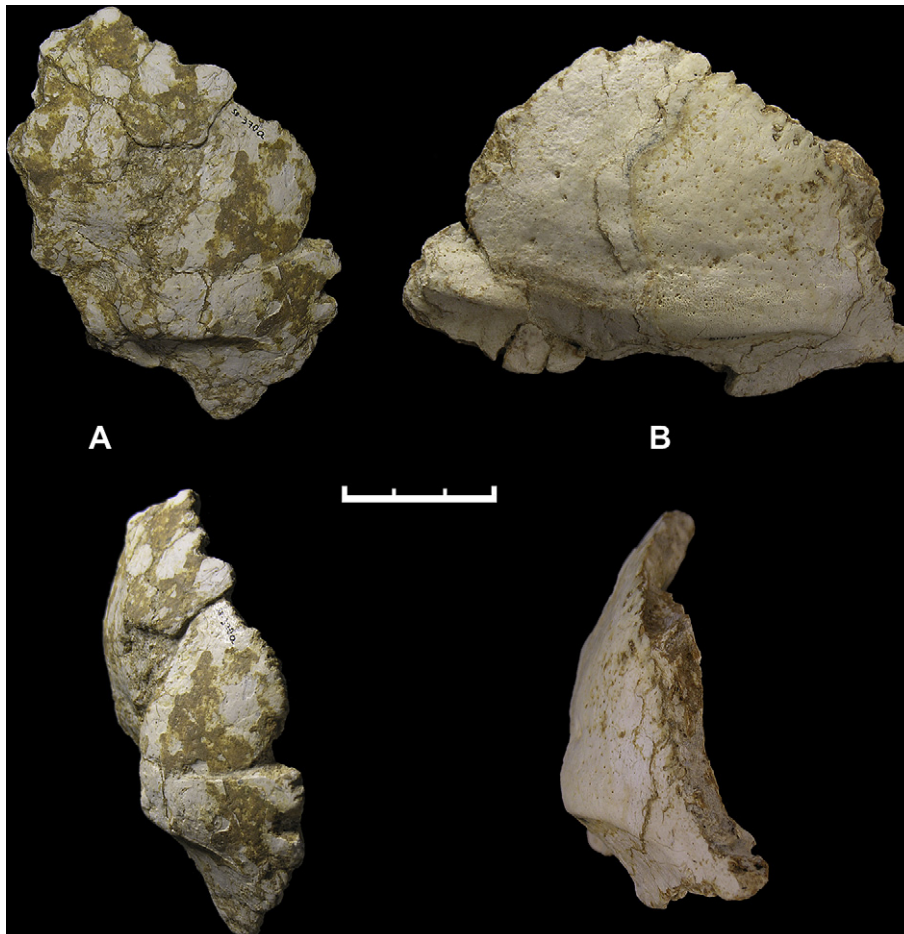

Figure 2. Original fossils in posterior (upper part) and lateral views (lower part). A) SD-370a, B) SD-1149. Scale bar is 3 cm.

2005, 2006). This definition is used in the present paper. Hublin (1984) suggested that a suprainiac porous area is sometimes also present in recent humans, but, morphologically, it is never as well-defined and extended as it is in Neandertals (Hublin, 1984; Caspari, 2005).

A juxtamastoid eminence occurs at the nuchal plane, medial to the relatively small mastoid processes, which projects inferiorly and beyond the mastoid process apices (Hublin, 1984, 1998; Arsuaga et al., 1997; Dean et al., 1998). This trait is "very typical" of Nean-dertals (Hublin, 1984:49), although not explicitly autapomorphic.

Another disputed feature on the occipital plane is a convexity ("chignon" or "occipital bunning") that strongly projects posteri-orly in the midline and shows some medio-lateral extension (Hublin, 1978; Trinkaus and LeMay, 1982; Smith and Trinkaus, 1991; Arsuaga et al., 1997; Churchill and Smith, 2000; Sládek, 2000; Gunz and Harvati, 2007). Following Trinkaus and LeMay, the 'chignon' is a "posterior projection of the occipital squama, which is evenly rounded in *norma lateralis* and slightly compressed in a craniocau-dal direction. The superior border of the occipital bun is along the lambdoid suture, and its inferior margin is in the region of the attachment of the *tentorium cerebelli*" (1982:27).

It has recently been shown that the morphology of the chignon in the midline is not unique to Neandertals (Gunz and Harvati, 2007). Nevertheless, these authors revealed that a relatively high position of a (more or less convex) occipital plane relative to the rest of the cranium typifies Neandertals. In this feature Neandertals differ from Upper Palaeolithic modern humans, which show a "hemi-bun" (Churchill and Smith, 2000) that is similar in midline curvature but in a different position relative to the rest of the skull (Gunz and Harvati, 2007).

Material and methods

The descriptive part of this paper concentrates on an overall morphological and anatomical description of the occipital fossils SD-1219, SD-1149, and SD-370a. We also assess phylogenetically meaningful features (e.g., Neandertal traits) of the external aspects of these specimens. Comparative data were obtained from high quality casts, CT-scans, and STL-models (Nespos, www.nespos.org), as well as from the literature (Hublin, 1984; Condemi, 2001; Caspari and Radovčić, 2006). For aims of comparability with other literature, traditional morphometrics were carried out using classical linear measurements (lambda-inion chord, biasterionic breadth, vault thickness, and suprainiac fossa diameters). Linear measurements were taken on the original fossils and casts by calipers measured to the nearest 0.5 mm and calculated from 3D landmarks on the 3D reconstructions and the digitised data. Further measurements were taken on CT slices with image software (Amira 4.1). Thickness at inion was measured orthogonally to a tangent on inion in a midsagittal CT-slice. Thickness at the superior occipital fossae was measured at the centre of the fossae in sagittal and axial slices. Suprainiac fossa breadth was measured at the edges of the fossa at its maximum diameter, and height was measured at the edges of the fossa in the midsagittal plane.

A total of two geometric morphometric shape analyses were conducted. Right and left asterion, inion, and lambda landmarks were used in the first shape analysis on a large comparative sample (Table 1, "full analysis"). In the second step of our shape analysis (Table 1, "semilandmarks analysis"), eight equally-spaced semi-landmarks were digitised for an assessment of the midsagittal curvature between inion and lambda. These additional data were taken on specimens attributed to the European Neandertal lineage in order to address local evolution in Europe as well as intra-specific Neandertal variation. Curve data were not available for the larger sample and thus not included in the full analysis (Table 1).

Table 1
Comparative sample used in this analysis. CT-data: computed tomography data; STL: virtual surface data; FA: full analysis; SL: semilandmarks analysis.

Fossil	Species	Data	Analysis
KNM ER-3733	*H. ergaster*	CT-data	FA
KNM ER-3883	*H. ergaster*	CT-data	FA
KNM WT-15000	*H. ergaster*	CT-data	FA
D2280	*H. ergaster*	Cast	FA
D2282	*H. ergaster*	Cast	FA
D2700	*H. ergaster*	Cast	FA
Ngawi	*H. erectus*	Cast	FA
Sambungmacan 1 (SM1)	*H. erectus*	Cast	FA
Sambungmacan 3 (SM3)	*H. erectus*	Cast	FA
Solo 6	*H. erectus*	Cast	FA
Solo 9	*H. erectus*	Cast	FA
Sangiran 17 (San17)	*H. erectus*	Cast	FA
Sangiran 2 (San2)	*H. erectus*	Cast	FA
Sangiran 4 (San4)	*H. erectus*	Cast	FA
Zhoukoudian	*H. erectus*	Cast[a]	FA
Ceprano	*H. antecessor*	Cast	FA
Cranium 5; Atapuerca Sima de los Huesos (Cr5)	*H. heidelbergensis*	Cast	FA, SL
Petralona	*H. heidelbergensis*	Cast	FA, SL
Reilingen	*H. heidelbergensis*	CT-data	FA, SL
Swanscombe (Swans)	*H. heidelbergensis*	CT-data	FA, SL
Steinheim	*H. heidelbergensis*	CT-data	FA, SL
La Chaise Bourgeois-Delaunay 6 (ChaiseBD6)	*H. neanderthalensis*	STL	FA, SL
La Chaise Suard 9 (ChaiseS9)	*H. neanderthalensis*	Cast	FA
Biache-St.-Vaast (Biache)	*H. neanderthalensis*	Cast	FA
Salzgitter-Lebenstedt (Salzgitter)	*H. neanderthalensis*	STL	FA, SL
Guattari 1	*H. neanderthalensis*	CT-data	FA, SL
Gibraltar 1 (Gib1)	*H. neanderthalensis*	CT-data	FA, SL
Spy 1	*H. neanderthalensis*	CT-data	FA, SL
Spy 2	*H. neanderthalensis*	CT-data	FA, SL
Amud 1	*H. neanderthalensis*	CT-data	FA, SL
Tabun C1 (Tabun)	*H. neanderthalensis*	CT-data	FA, SL
La Chapelle-aux-Saints 1 (Chapelle)	*H. neanderthalensis*	CT-data	FA, SL
La Ferrassie 1 (Fer)	*H. neanderthalensis*	CT-data	FA, SL
SD-1219	*H. neanderthalensis*	Original	FA, SL
Saccopastore 1	*H. neanderthalensis*	Cast	FA, SL
L'Abri Pataud	*H. sapiens*	Cast	FA
Chancelade	*H. sapiens*	Cast	FA
Cro-magnon 1	*H. sapiens*	Cast	FA
Mladeč 1	*H. sapiens*	CT-data	FA
Jebel Irhoud 1 (Irhoud)	*H. sapiens*	Cast	FA
Ngaloba (LH18)	*H. sapiens*	Cast	FA

[a] "Weidenreich/Swan" skull reconstruction (Tattersall and Sawyer, 1996).

Landmark data from fossils and casts were collected using MicroScribe 3DX and G2 digitisers, with landmark 3.0 software (http://graphics.cs.ucdavis.edu) used to measure 3D landmarks on the 3D computer reconstructions (Wiley et al., 2005). Curve land-mark data collected with the MicroScribe were resampled using resample-software (http://research.amnh.org/nycep/nmg) in order to produce data sets with the same number of equally-spaced semilandmarks. The semilandmarks were then slid along their tangents so as to minimize bending energy between the consensus and each of the specimens (Gunz and Harvati, 2007).

Geometric morphometrics and statistical analyses

Standard Procrustes methods were used for shape analysis (Rohlf and Slice, 1990; Bookstein, 1991; O'Higgins, 2000). During generalized Procrustes analysis, the landmark configurations are translated to common origin, scaled to unit centroid size, and then rotated iteratively according to a best-fit criterion that minimizes overall Procrustes distance. Centroid size is used as a size measurement (i.e., the square root of the sum of squared distances of all landmarks to the centroid of the object). The metrics of shape are Procrustes distances (d), defined as the square root of the

summed squared distances between Procrustes registered landmark configurations (Bookstein, 1991).

Shape and size data were obtained and analysed by Principal Components Analysis and regression analysis using Morphologika 2.5 software (O'Higgins, 2000). Cluster analyses (minimum spanning tree) of Procrustes distance matrices were carried out by NTSys PC2.2 (Rohlf, 1997) and Statistica 6.0 for PC (StatSoft, 1999).

Results

Morphological description of SD-1219

The SD-1219 fossil comprises most of the posterior part of a cranial vault and base, with the left side being better preserved than the right (Fig. 1). The left half of the occipital bone is virtually complete, although the nuchal plane area is partially reconstructed from small fragments. The occipital squama is broken close to lambda, which is not preserved. However, the position of lambda can be estimated by extrapolation of the lambdoid suture to the midline. Adjacent to the occipital is a left petrous temporal, which is complete except for the petrosal apex medial to the internal acoustic porous, and a small portion of the left parietal. The left mastoid portion is relatively complete but eroded. A portion of the right half of the occipital bone is missing, and it has a diagonal fracture that runs obliquely from close to lambda, passing laterally to the right lateral bulge of the transverse occipital torus, towards the nuchal plane. A thin layer of sedimentary matrix covers the surface along the fracture on the right half of the fossil.

The right part of the basi-occiput is preserved and the left part could be anatomically fitted during the restoration process. This reconstruction permits localisation of opisthion, and an assessment of a relatively large foramen magnum. The anterior part of the occipital base, and thus basion, could not be reconstructed.

All the sutures (left parieto-mastoid and occipito-mastoid suture) are clearly discernible and unfused. The lambdoid suture is also open, suggesting that this individual was a young adult. A Wormian bone occurs in the lambdoid suture approximately 20 mm medially from asterion. The external surface of the bone is smooth but shows some porosity at the occipital plane. The nuchal plane is relatively smooth and shows no porosity.

The occipital plane displays a marked convexity, which results in a marked occipital bunning, inferiorly demarcated by a well-defined transverse occipital torus. In spite of missing parts, a certain lambdoid flattening can be appreciated in the specimen. This morphological combination clearly reflects the anatomy of the "chignon" often found in classic Neandertals.

A characteristic suprainiac fossa is identified in SD-1219, centred on the occipital plane just superior to the occipital torus. The suprainiac fossa is oval in form with a distinctive porous surface. It is relatively broad (Table 2), largely shifted towards the left, and follows the overall asymmetric pattern of this individual (Rosas et al., 2008). The suprainiac fossa is delineated superiorly by the upper lip of the transverse occipital torus; the supreme nuchal line, according to Hublin (1978).

The transverse occipital torus in SD-1219 is conspicuously defined topologically as a marked step between the occipital plane and the nuchal plane. Inferiorly, the torus becomes accentuated by the depth of the semispinal muscle fossae. The transverse occipital torus occupies the central part of the occipital squama, extending laterally from the midline about 50 mm. The lateral end of the torus disappears rapidly without continuity into the most lateral area of the occipital squama, and can be located in a parasagittal plane roughly coincident with the cranial end of the Waldeyer's crest. In rear view, the torus presents a wide central area of triangular shape that is thicker vertically, which becomes thinner when approaching the lateral parts of the occipital bone. The occipital torus is relatively thick, and a superior and an inferior lip can be identified. The superior lip is less clearly marked than the lower lip of the torus, which is better defined in the central area where it establishes the lower side of the suprainiac fossa. The superior nuchal line is clearly marked as the inferior lip of the torus (Feneis, 1982) and becomes smoother towards the midline, where it curves bilaterally caudally, giving origin to a smooth external occipital crest. This configuration produces a triangular surface (mentioned above) on which the linear tubercle can be identified.

In superior view, the occipital transverse torus is straight but smoothly depressed in the midline area, creating a bilaterally protruding torus; a configuration typical of Neandertals (Hublin, 1978, 1998). The lateral portion of the torus, which is better appreciated in the preserved left side of SD-1219, forms a distinctive bulging in continuity with the proximate portion of an inflated

Table 2
Neandertals, linear measurements (mm). (1) Caspari and Radovčić, 2006; (2) Condemi, 2001; (3) Hublin, 1984.

Fossil	Bi-asterionic breadth M12	Lambda-inion M31(1)	Lambda-asterion M30(3)	Inion-asterion	Inion thickness	Superior occipital fossae		Suprainiac fossa locus	
						Left	Right	Breadth	Height
SD-1149		59			12	5	6	42	12
SD-1219	120.6	59.4	90.4	68.7	13	4	6	40	12
Krapina 5		61.6 [1]	86.3 [1]	71.8 [1]	12 [1]			34 [1]	17 [1]
La Chapelle-aux-Saints 1	126.1	60.6	93.3	71.6	9	7 [3]	8 [3]	39	10
La Ferrassie 1	121.6	59.5	89.6	68.6	10	5 [3]	6 [3]	32	16
Guattari 1	120.7	63.1	94.3	67.7	11	7	6	48	10
Feldhofer (Neandertal 1)		59.0 [2]			13	6	6	40	11
La Chaise Suard 9	111.0 [3]	55.0 [3]							
La Chaise Bourgeois-Delaunay 6	112.3	61.2	76.9	57.1	10	6 [2]	5 [2]	51	20
Saccopastore 1	109.7	57.5	92.5	67.3					
La Quina H5	112.0 [3]	60.0 [3]							
Spy 1	113.3	58.9	90.7	66.8	13	6	6	32	14
Spy 2	122.6	60.0	89.7	70.7	11	4	4	47	19
Salzgitter-Lebenstedt	117.5	60.5	79.9	71.3		6 [3]	6.5 [3]	44	9
Gibraltar 1	98.0	57.4	86.2	67.7	10	5	6	25	15
Tabun C1	107.0	56.5	79.6	63.5	6	5	5	37	16
Mean	114.3	59.3	87.2	67.6	10.5	5.7	5.9	39.0	14.3

occipital plane, clearly expressing an occipital bunning. The lateral area of the left semispinal muscle region shows an infratoral sulcus. The most projecting point of the occipital torus coincides with the deepest point of the occipital fossa at the internal side.

The nuchal plane is characterised by muscle insertions with two morphologically well-differentiated regions. The inferior nuchal line is, however, poorly defined. The upper portion of the nuchal plane is mostly dominated by the attachment for the semispinalis capitis muscle, while the less-preserved lower part presents a more complicated relief.

The semispinalis capitis muscle leaves two deep, asymmetric fossae that are separated in the midline by a wide and smooth external occipital crest. Furthermore, the external occipital crest deviates from the midsagittal plane slightly towards the left in a caudal direction.

The insertion area of the semispinalis muscle shows an asymmetric disposition, and, inside the larger area of attachment, two smaller bilateral fossae are clearly distinguished. The right fossa is larger and elongated ($\sim$24.5 mm long), and runs roughly parallel to the occipital torus. The left fossa is smaller ($\sim$21 mm) and runs more obliquely with respect to the torus. More caudally, the semispinalis muscle area appears as an inflated prominence that extends over the area corresponding to the inferior nuchal line.

The region of the nuchal plane occupied by the deep neck musculature presents a complicated relief. The midline region is mostly missing and the right side is incomplete. Nonetheless, the following features can be securely assessed. On the right side, a shallow but wide depression can be appreciated, topologically corresponding to the muscle markings of the posterior minor rectus capitis muscle. Such a depression cannot be observed on the left side.

At the left lower part of the nuchal plane, there is a well-marked Waldeyer's crest, which is oriented in a para-sagittal plane, suggesting strong development of the oblique capitis superior muscle. This crest has been suggested to be more strongly developed in Neandertal males than females (Smith, 1980), although such marks are generally smoother in Neandertals than in modern humans (Caspari and Radovčić, 2006). The occipital lip of the juxtamastoid crest extends cranially, running parallel to the Waldeyer's crest, producing between them a wide sulcus (13.5 mm) topologically corresponding to the attachment area of the superior oblique muscle.

The condylar sulcus is deep and long, running obliquely from the medial to the rear part of the condyle. This sulcus is very well-delineated superiorly and laterally by a conspicuous crest, which runs parallel to this sulcus.

The basilar part is heavily fragmented, but some isolated features can be assessed. The foramen magnum is incomplete, although an elongated shape approximately 45 mm long and 36 mm wide may be clearly appreciated. While the left condyle is eroded and mostly missing, the right condyle is nearly complete. The preserved condyle is large (approx. 22.5 mm × 18 mm). Its surface is flat, with an irregular perimeter, wider at its distal end, and without a neat elevation. The jugular foramen is large. A wide and lengthened hypoglossal canal runs obliquely in an angle close to 45° relative to the sagittal axis of the foramen magnum.

The clivus is only represented by a small portion and preserves marks for the insertions of the prevertebral musculature. Specifically, a prominent, laterally orientated tubercle marks the attachment of the rectus capitis anterior muscle.

Preservation and morphological description of SD-1149

The SD-1149 occipital fragment consists of a major part of the occipital plane, and includes a small superior portion of the nuchal plane (Fig. 2). In general terms, the exo- and endocranial surface morphologies of the fossil are well-preserved. Superiorly, the bone is broken close to lambda, the position of which can be roughly estimated following the trajectory of the right lambdoid suture. This suture shows a characteristic lobulated morphology. The left part of the occipital plane is partially missing. An oblique fracture runs from close to lambda until approximately 40 mm lateral to the midline at the caudal limit of the bone. The lower left part of the occipital plane is also crushed diagenetically.

The symmetry of the bone is defined by the internal occipital protuberance and internal sagittal crest. The curvature of the occipital plane is low, being almost flat in the portion closer to the occipital torus. There is no development of a chignon.

The external bone surface shows a certain degree of porosity. The occipital insertions of the m. epicranius fibres can be well-recognized as little vertical grooves located cranially to the smooth bony lip of the transverse occipital torus (i.e., supreme nuchal line [Hublin, 1978]). The linear tubercle is only slightly marked and no strong external occipital protuberance is observed. The morphology of the transverse occipital torus shows a marked bilateral protrusion and it is clearly depressed in the midline, where the torus almost disappears.

Superior to the transverse occipital torus, a long and shallow sulcus can be identified that is approximately 42 mm broad and 12 mm high (Table 2, Fig. 2). Despite its anatomical position, this sulcus does not look like a typical suprainiac fossa *sensu stricto* such as observed in SD-1219 or other Neandertals. This is because the surface texture of the suprainiac fossa does not differ from the surface texture of the surrounding bone. In addition, the shape does not demarcate a typically oval or elliptic outline.

Though incomplete, a wide semispinalis muscle fossa can be appreciated on the right side. It is superiorly well-defined by the sharp lower edge of the occipital torus.

Preservation and morphological description of SD-370a

The SD-370a occipital is a fragmented right half of an occipital squama (Fig. 2). The bone is deformed and its surface shows several cracks due to post mortem taphonomy. However, despite these surface alterations the fossil preserves some important details of morphology.

On the external surface, parts of the right lambdoid suture are preserved from in proximity to lambda until approximately 24 mm superior to the right extreme of the transverse occipital torus. The right half of the transverse occipital torus is entirely preserved and displays a clear posterior projection, which is most pronounced 15 mm off the midline. This projection corresponds to the right bulge of an originally bilaterally protruding torus. Towards the midline the torus profile disappears. The linear tubercle is not preserved because of a fracture. The lateral end of the torus terminates in the form of a thin but clearly discernible line that is curved latero-inferiorly.

In the midline, there is a relatively deep and slightly vertically elongated depression, most probably formed by taphonomic compression. This circular depression does not correspond to a suprainiac fossa. Inferior to the transverse occipital torus, a small part of the nuchal plane is preserved corresponding to the portion of the semispinalis capitis muscle attachment.

In lateral view, the bone is relatively flat. This is better assessed in a parasagittal region than in the midline, where the bone is deformed and cracked, producing – artificially- an impression of stronger convexity. When compared to other Neandertal occipitals, the fossil is long superior to inferior (estimated lambda-inion chord is 65 mm), but narrow and thin, possibly indicating a young individual.

Virtual reconstruction of SD-1219

For the digitisation of the SD-1219 landmarks, several possibilities for missing data reconstruction were explored, including statistical, geometric, and anatomical methods (Gunz et al., 2004). Among the anatomical methods, bilateral symmetry is of primary importance. "Reflected relabelling" (Mardia et al., 2000) makes use of Procrustes geometry in order to reflect paired landmarks without the necessity of defining a symmetry or mirroring plane. However, in the case of SD-1219, reflected relabelling could not be carried out because corresponding bilateral landmarks are not preserved. Only left asterion is present. Additionally, no consistently reproducible midline could be defined and used for mirroring of asterion in order to compensate for the lack of bilateral landmarks. This is because of morphological asymmetry: at the exocranial part, an asymmetric position of the suprainiac fossa was observed. On the endocranial side, a pronounced occipital petalia and an associated torsion cause a deviation and lateral shift of the falx cerebri attachment from the midline (Rosas et al., 2008). Altogether, these factors precluded a reliable and rigorously reproducible estimate of the curvature landmarks at the midsagittal plane.

Thus, the specimen was reconstructed virtually by mirroring the 3D model of the fossil and merging it with its reflected counterpart, maintaining the nuchal plane of the original fossil (Fig. 1). For the mirroring process, bilateral geometrical symmetry was considered, with the aim of preserving a homogeneous curvature at the exocranial occipital surface in axial view. Repeated reconstructions of SD-1219 gave very similar medio-lateral dimensions (<1%). Validation of this reconstruction method was also carried out by a simulation study. We virtually removed the right posterior half of the braincase from a 3D reconstruction of the La Ferrassie 1 Neandertal created from CT-scans to obtain a fragment anatomically similar to SD-1219. Repeated reconstructions of this "virtual fragment" gave, on average, a deviation of approximately 5.6% less than the original bi-asterionic diameter.

This anatomical reconstruction method provided a morphologically smooth external occiput and a reliable position of right asterion (Fig. 2). After that, only the position of lambda needed to be estimated, which was straightforward following the natural anatomical curvature of the lambdoid suture and assuming

a continuous trajectory, as is the case in most Neandertals (except La Chaise Bourgeois-Delaunay 6) (Condemi, 2001). The SD-370a and SD-1149 occipitals have presently been excluded for shape analysis.

Linear distances

In many features the El Sidrón occipitals show values close to the average measurements of the comparative Neandertal sample (Table 2 and Fig. 3). Cranial thickness of the El Sidrón occipitals matches those of other Neandertals, but the El Sidrón specimens are slightly above the overall Neandertal mean. However, thickness at inion is particularly high in SD-1219, a feature resembling Spy 1 and the Feldhofer specimen. The heights of the upper scale (lambda-inion chord) of SD-1149 and SD-1219 fall close to the Neandertal mean (Table 2, Fig. 3). The breadth of the suprainiac fossa in these occipitals tends to be slightly above the mean.

Geometric morphometric shape analysis

The principal components analysis in Fig. 4 is based on 3D coordinates of four landmarks (right and left asterion, lambda, and inion), which reflect the major spatial proportions of the occipital plane, and capture overall variation in the bone. PC1 and PC2 account for 82% of the total variance. Morphologically, PC1 reflects a gradient separating primitive and derived states in the genus *Homo*, with relatively broader and lower occipitals on the negative scores (*H. erectus*, *H. ergaster*) and narrower and higher occipitals on the positive scores (modern humans, Neandertals, and Middle Pleistocene humans). Towards the positive end of PC1, the scores of PC2 polarize Neandertals on the positive loadings and modern humans on the negative loadings. Morphologically, these distributions reflect variation in the relative height and position of the occipital scale and the relative vertical distance of inion to the bi-asterionic axis. In Neandertals, the entire occipital plane is elevated and shifted posteriorly with respect to the bi-asterionic axis. In contrast, inion is lowered in modern humans towards the same vertical level as the bi-asterionic axis and shifted anteriorly.

In the PC1-PC2 subspace of Fig. 4, SD-1219 plots slightly off the centre, in the shape vicinity of Solo 6 and Dmanisi 2280 on the left, and Gibraltar 1, Spy 2, and La Ferrassie 1 on the right. The polygon in Fig. 4, which includes all the Neandertals, shows that, within Neandertals, SD-1219 is closer to La Chaise Bourgeois-Delaunay 6 and to Salzgitter-Lebenstedt. This limit of Neandertal variation is also closer to the primitive morphological pattern of *Homo* (*H. ergaster*, *H. erectus*, and Petralona [*H. heidelbergensis*]). Consequently, these Neandertals show broader and lower occipitals than those on the other end of the distribution. Regression analysis indicates that PC1 shows a very slight, but statistically significant allometric component ($b = 0.0037$, $p = 0.015$). This suggests that allometry is likely of little relevance in occipital plane evolution.

A semilandmarks analysis of occipital plane morphology in the European Middle Pleistocene

The second shape analysis was performed using semilandmarks that were slid along the midline occipital plane, and fossils exclusively attributed to the European Neandertal lineage (e.g., *H. heidelbergensis sensu* Rosas and Bermúdez de Castro [1998], and *H. neanderthalensis*) (Fig. 5). The associated morphological patterns indicate that occipital morphologies that are relatively low and broad fall on the positive end of PC1, whereas higher and narrower occipitals are observed on the opposite end. A Minimum Spanning Tree (MST) based on the full shape space rather than on some restricted projections is plotted in Fig. 5. The closest neighbour of SD-1219 in the MST is Cranium 5, which also links to Petralona, La Chaise
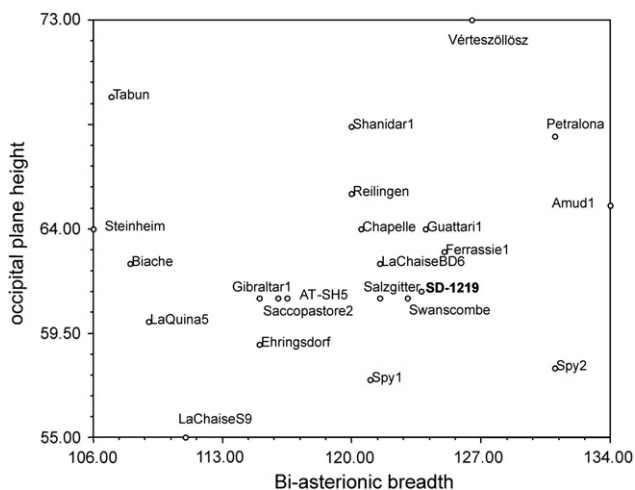
Figure 3. Scatterplot of bi-asterionic breadth (mm) and occipital plane height (lambda-inion chord) (mm) in European Middle Pleistocene fossils. SD-1219 is in the vicinity of Salzgitter-Lebenstedt ("Salzgitter"), Swanscombe, and La Chaise Bourgeois-Delaunay 6. It plots on the right side, which indicates that SD-1219 (in bold) tends to be broader with a slightly decreased lambda-inion chord. (Data from Table 2, otherwise from Condemi [2001].)
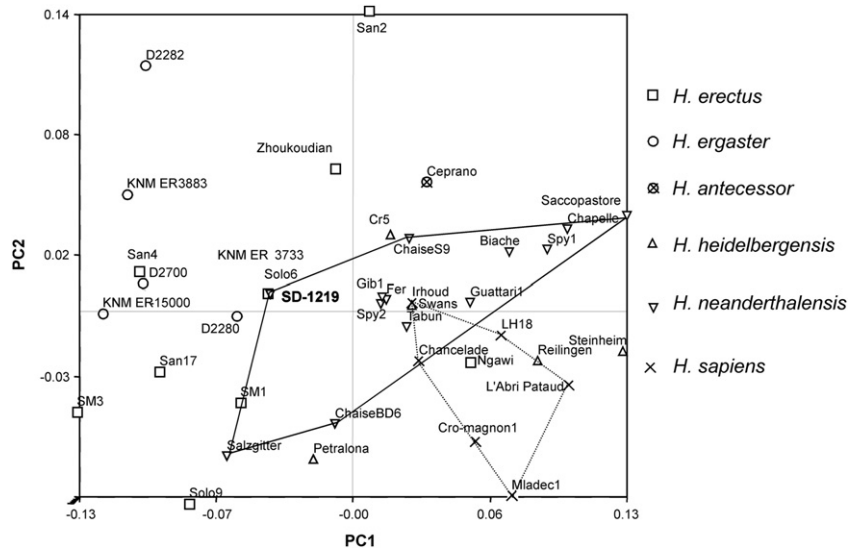
Figure 4. Scatterplot of PC1 and PC2 scores for the large comparative sample. These scores are calculated using four 3D landmarks (right and left asterion, lambda, inion). SD-1219 (in bold) plots slightly off the centre and closer to the primitive morphological patterns. The large solid polygon encloses Neandertal variation, in which SD-1219 plots on one extreme together with Salzgitter-Lebenstedt and La Chaise Bourgeois-Delaunay 6. The small dotted polygon encloses fossil *H. sapiens* variation in this projection. Abbreviations as in Table 1.

Bourgeois-Delaunay 6, and Tabun C1, linking with Gibraltar 1 and Spy 2. This grouping is similar to the first PCA in the full hominin sample, which is based on fewer landmarks, where SD-1219 was closer to Spy 2, Swanscombe, La Ferrassie 1, Tabun C1, and Gibraltar 1.

Because our results revealed both male and female Neandertals in the shape vicinity of SD-1219, a geometric morphometric shape analysis of 120 modern human occipitals was conducted for comparative purposes. This analysis showed no statistical evidence for sexual dimorphism in shape in the modern human population (permutations of mean shape comparisons, $N = 1000$, $p > 0.05$), while centroid size was highly significantly different ($p < 0.001$), suggesting that size is an important sex-specific feature. Centroid size (CS) for SD-1219 (CS = 122.1) is above the Neandertal mean (CS = 120.8).

Finally, a cluster analysis was performed on the Procrustes distance matrix (Fig. 6). The associated UPGMA-tree suggests three different clusters: 1) one fraction including Petralona and Salzgitter-Lebenstedt; 2) a larger intermediate fraction, which contains SD-1219 clustering with La Chaise Bourgeois-Delaunay 6, Cranium 5, Tabun C1, Gibraltar 1, La Ferrassie 1, Spy 2, Swanscombe, and Amud 1; and 3) a smaller fraction including Spy 1, Guattari 1, La Chapelle-aux-Saints 1, and Saccopastore 2.

Discussion

The aim of this study was a morphological assessment of the occipital bones of the El Sidrón hominins (Rosas et al., 2006) and an evaluation of their evolutionary position. Our investigation was guided by the following research questions: 1) What is the phylogenetic status of the El Sidrón occipitals? and 2) How does El Sidrón occipital morphology contribute to understanding intraspecific variation in Neandertals?

The phylogenetic status of the El Sidrón occipitals

The descriptive morphological analysis has shown that all of the El Sidrón fossils, SD-1219, SD-1149, as well as SD-370a, display autapomorphic Neandertal features. Apparently, SD-370a shows a morphology that resembles a bilaterally transverse occipital torus, which is also clearly recognisable in SD-1149. However, in SD-1149,

a flat morphology of the occipital plane indicates a lack of occipital bunning. The SD-1219 occipital presents the listed Neandertal autapomorphies as well as other traits that are very typical of Neandertals (e.g., chignon, juxtamastoid eminence). The fact that SD-1149 and SD-1219 differ with respect to occipital bunning supports the argument of Trinkaus and LeMay who suggested that "as with most of the features of the cranium, there is a morphological continuum between complete absence and full development of a bun [...]. It is therefore not possible to decide dichotomously for all crania whether an occipital bun is present" (1982:28).

A similar statement could be made regarding the diagnosis of the suprainiac fossa, which shows a typically oval Neandertal morphology in SD-1219 but apparently not in SD-1149. While there is a depression above inion in SD-1149, which can be measured approximately (Table 2), it is sulcus-like and very different in morphology compared with other, typical Neandertal suprainiac fossae (Hublin, 1984; Caspari, 2005). Also, the lack of differences in surface porosity between the suprainiac sulcus and its surrounding area in SD-1149 suggests a certain distinctiveness of SD-1149. Future study should investigate this problem in more detail.

The results in Fig. 4 illustrate quite clear morphological trends separating early *Homo*, the Neandertal lineage, and fossil *H. sapiens*. This is interesting because other studies did not distinguish unambiguously between Neandertals and modern humans (Spitery, 1985; Harvati, 2001) and these differences in findings might be related to methodological issues. For example, Spitery (1985) used traditional measurements, which, unfortunately, do not consider spatial aspects of morphology such as the relative elevation of the occipital plane relative to left and right asterion captured by 3D geometric morphometrics. However, Harvati (2001), who also conducted a 3D geometric morphometric study, could not identify these configurational features. This is likely related to the fact that Harvati (2001) used a broader comparative sample. Particularly, the inclusion of chimpanzees in her study likely shifted the weight of the distributions along the principal components. A later study including only humans combining midline and lateral cranial landmarks gave clearer separations (Gunz and Harvati, 2007), which are similar to the present findings.

Finally, the number and distribution of landmarks could be important. Spitery (1985) stated that the occipital squama is

particularly informative about evolutionary trends in *Homo*, whereas she suggested that the nuchal plane mainly reflects bipedal locomotion. Thus, landmarks at the nuchal plane might add some "noise" and contribute to a less clear separation of human species in occipital studies. This could be another reason why our study, using four landmarks on the evolutionary "more informative" part of the occipital (Spitery, 1985), finds clearer separation between Neandertals and modern humans. In this respect, it is similar to a recent study on basicranial evolution in which clear signals were found using six landmarks in an evolutionary "very informative" region (Bastir et al., 2008).

Another interesting finding of this study is shown in Fig. 4, which orders the specimens - to some degree - from a more primitive morphology (relatively lower and wider occipital planes) on the negative PC1 scores to a more derived morphology on the positive PC1 scores (relatively higher and narrower occipital planes). This
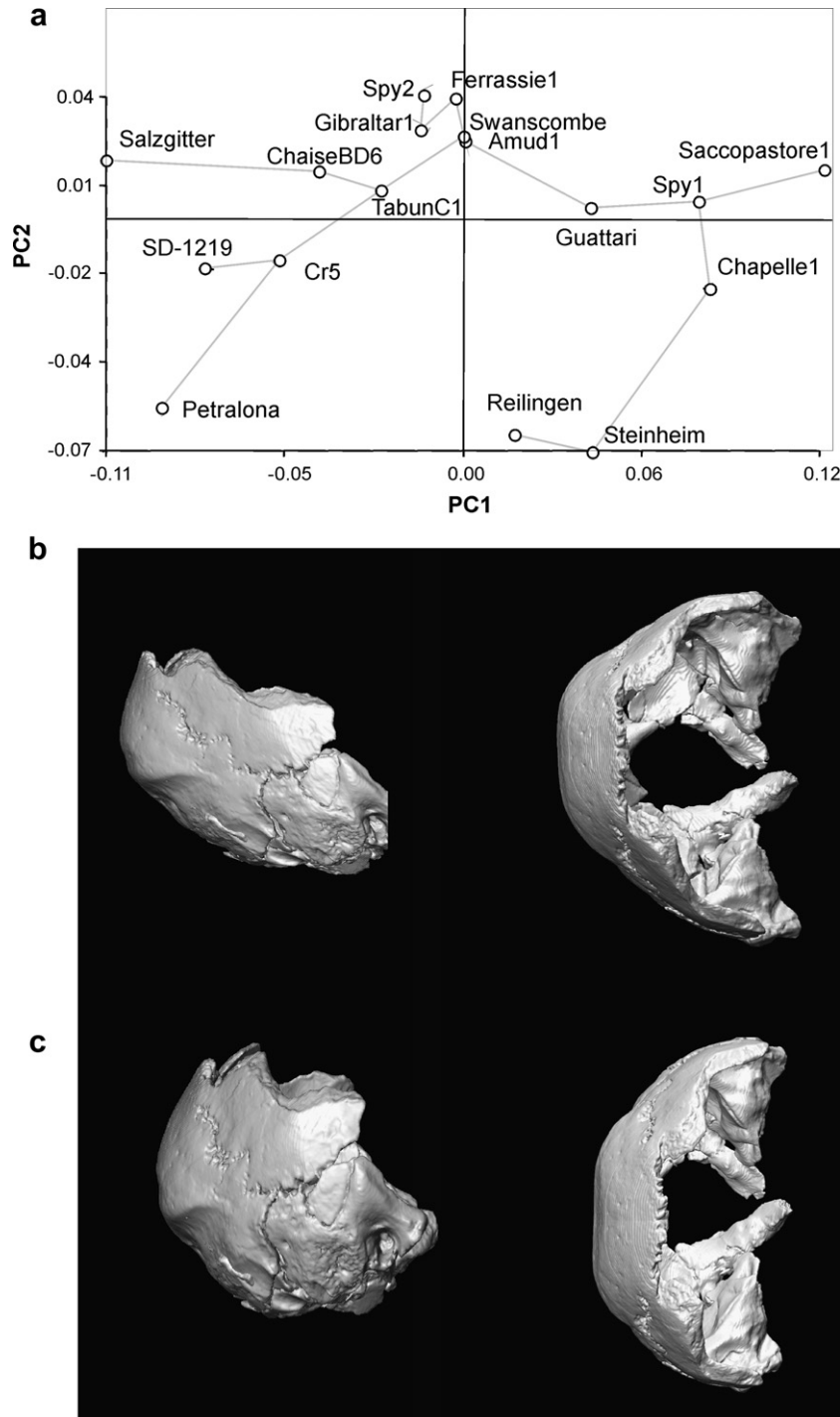

Figure 5. Semilandmarks analysis of Neandertal lineage only. a) Scatterplot of PC1 and PC2 and Minimum Spanning Tree (MST). The thin grey line of the MST indicates the closest neighbours in terms of Procrustes distance, calculated in full shape space to each specimen. SD-1219 connects with Cranium 5, which links with Petralona and Tabun C1. PC1 describes intraspecific morphological variation in Neandertals. This variation is shown in the lower part of the figure (b and c) as a surface model of the SD-1219 specimen warped onto the positive and negative extremes of PC1. b) Positive loadings; c) negative loadings. Note the narrower and more elongated posterior braincases with strong posterior projection (b) corresponding to positive PC1 scores versus relatively broader, shorter braincases with less posterior projection corresponding to negative PC1 scores.
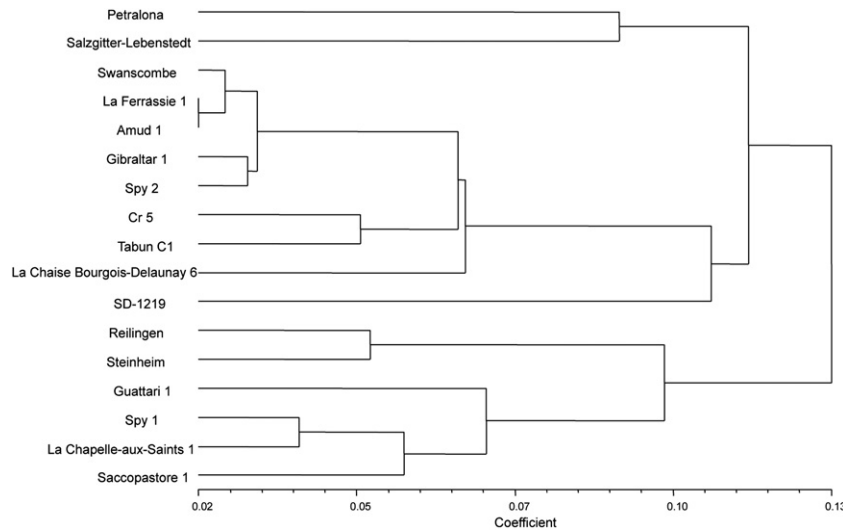
Figure 6. UPGMA tree based on Procrustes distance (d) of slid semilandmark data. One cluster includes Petralona and Salzgitter-Lebenstedt; a larger intermediate one includes SD-1219 clustering with La Chaise Bourgois-Delaunay 6, Cranium 5, Tabun C1, Gibraltar 1, La Ferrassie 1, Spy 2, Swanscombe, and Amud 1; and a third cluster includes Spy 1, Guattari 1, La Chapelle-aux-Saints 1, and Saccopastore 2.

factor could be evolutionary in nature, i.e., interspecific, and might refer to overall cranial size. Hominins with smaller neurocrania (e.g., *H. ergaster*, *H. erectus*) tend to plot on the left side of PC1, while larger brained hominins tend to plot on the right side (e.g., Neandertals, *H. sapiens*) (Ruff et al., 1997; Rightmire, 2004). Also, the subtle allometric signal could be interpreted in this direction but should be taken with caution.

However, the results of the PCA in Fig. 4 suggest that intraspecific variation is also important to consider in similar geometric terms. In this respect, it seems interesting to mention that SD-1219 is closer to one end of the Neandertal distribution, with relatively lower and broader proportions (Figs. 4 and 5). Thus, the evolutionary trend of ordination overlaps to some degree with an intraspecific trend of ordination particularly within the Neandertal lineage.

This overlapping distribution in Fig. 4 might be compatible with a recent study addressing the usefulness of the different cranial bones for reconstructing population history (von Cramon-Taubadel, 2009). Von Cramon-Taubadel found that the occipital deviated most from neutral genetic evolutionary expectations (von Cramon-Taubadel, 2009). Figure 4 could be interpreted in this direction. However, von Cramon-Taubadel's suggestion to exclude occipital morphology from phylogenetically oriented studies should be taken with some caution until more research including morphological features other than landmarks, such as surface details and non-metric morphological features on the occipital (Hublin, 1978, 1984; Santa Luca, 1978; Arsuaga et al., 1997; Dean et al., 1998), is carried out in more detail (von Cramon-Taubadel, 2009).

Neandertal intraspecific variability

An evolutionary interpretation of the ordination on PC1 alone is not sufficient (Fig. 4), and additional intraspecific factors, driven by other aspects than cranial size, should be taken into account. One such factor is expressed by broader/lower versus narrower/higher braincases. This can be interpreted by combining the findings of Figs. 4 and 5, which both show that SD-1219 is relatively broader, shorter, and with less occipital plane elevation similar to Salzgitter-Lebenstedt (Hublin, 1984) and La Chaise Bourgeois-Delaunay 6 (Condemi, 2001), and different from other Neandertals, such as Guattari 1, or La Chapelle-aux-Saints 1.

This proximity to some potentially older Neandertals (Condemi, 2001) is also interesting given the relatively recent age of the El Sidrón fossils at 49 ka (Torres et al., in press). Neandertals that are roughly contemporary with El Sidrón plot at the other extreme (La Chapelle-aux-Saints 1, Guattari 1) (Figs. 4 and 5).

In a recent study, Rosas and colleagues interpreted intraspecific variation in Neandertals in terms of geographic variability (Rosas et al., 2006). In particular, their 3D geometric morphometric analysis showed that Neandertal mandibles from the north tended to be slightly - although statistically significantly - more elongated, and lower and narrower, while Neandertal mandibles from the south were antero-posteriorly shorter, and relatively higher and broader (Rosas et al., 2006). However, our occipital data offer no clear geographic signal (Fig. 5). This result may be related to the fact that, for developmental reasons, facial structures co-vary with basicranial ones in those anatomical regions where they are attached, that is, via the maxillary and mandibular connections to the external cranial base (Enlow, 1990; Bastir et al., 2004; Bastir and Rosas, 2006; Bastir et al., 2007; Bastir, 2008). The occipital is located posterior to the mandibular attachment. This part of the braincase needs not necessarily follow facial patterns and attendant facial variation related to geographic distribution (Enlow, 1990). Instead, the morphometric interpretation of the El Sidrón occipitals fits with the observations of Gunz and Harvati (2007), who reported similar integration patterns in Neandertals and modern humans that are morphologically expressed in terms of cranial sphericity. These authors related occipital shape variation with brain and braincase shape rather than to brain size, an interpretation that likely applies to our observations. Future study should address these important questions in more detail.

Sexual dimorphism presents another important aspect of intraspecific variation (Frayer and Wolpoff, 1985; Rosas and Bastir, 2002; Rosas et al., 2002). Unfortunately, little is known about sexual dimorphism in Neandertal crania, but principles similar to modern humans can be assumed: size and robusticity have been suggested (Smith, 1980), but these aspects have mainly been related to facial features. Smith (1980) suggested that facial size and browridge robusticity would be increased in Neandertal males compared with females. In mandibles of Neandertal ancestors, similar factors have been used for sex assignment (Rosas et al., 2002). On the occipital bone, two aspects have been mentioned: the robusticity of the insertion of muscle marks at the nuchal plane (Smith, 1980) and the

overall size and thickness of the occipital bone (Caspari and Radovcić, 2006). Trinkaus and LeMay (1982) did not exclude the possibility of sexual dimorphism in occipital morphology (e.g., bunning) in Neandertals. Our analysis of comparative data in modern humans did not reveal evidence for sexual dimorphism in occipital convexity.

In a similar sense, but from a metric perspective of size, the "mean method" (Rehg and Leigh, 1999; Rosas et al., 2002) suggests that measurements from individuals above the mean tend to be from males, while those below tend to be from females. Applying this approach to measures of cranial thickness suggests that both SD-1149 and SD-1219 are males (Table 2). Both fossils are thicker than Gibraltar 1 or Tabun C1, both of which are commonly accepted as female Neandertals. Furthermore, SD-1149 and SD-1219 are also thicker than a recently defined Neandertal male from Krapina, K5 (Caspari and Radovcić, 2006), and both exceed the mean of our comparative sample (Table 2). In addition, SD-1219 shows well-defined muscle insertion marks at the nuchal plane, a feature suggested by Smith (1980) to be sexually dimorphic, even though it has been recognised that these muscle markings are usually less pronounced in Neandertals than in modern humans (Caspari and Radovcić, 2006). Finally, in terms of centroid size, SD-1219 (CS = 122.1) slightly exceeds the Neandertal mean (CS = 120.8). Altogether, the evidence suggests a male Neandertal of intermediate size. If true, then each of the occipitals would correspond either to masculine individuals 1 and 2 as assessed from the mandibles (Rosas et al., 2006) or to another masculine individual.

It has been suggested that degree of pocking (porosity) is related to remodelling activity associated inversely to bone thickness, and has also been used as relative age indicator (Caspari, 2006). This suggests that the smooth surface of SD-1149 relates to an older individual, while the porous surface of SD-1219 represents a younger one. However, the El Sidrón occipitals are equally thick and thus deviate from the trend suggested by Caspari (2006).

Conclusions

This study has shown that the occipital morphology of the El Sidrón hominins displays typical differential diagnostic features of Neandertals. Descriptive morphology and linear measurements suggest that SD-1149 and SD-1219 are males, a diagnosis which obviously shares the well-known difficulties of sex assignment in fragmentary fossil hominin material. The surface features related to porosity could imply that SD-1149 and SD-1219 are adults not too advanced in age, and the apparent gracility in SD-370a suggests an immature individual. In addition, the geometric morphometric evidence suggests that SD-1219 is a male with a relatively broad and anteroposteriorly short braincase morphology, which would also fit the morphological patterns of either mandible 1 or 2 (Rosas et al., 2006). Future analysis will shed further light on these fossils, which belong to the most important Neandertal collection in the Iberian Peninsula.

Acknowledgements

References

Arsuaga, J.L., Martínez, I., Gracia, A., Lorenzo, C., 1997. The Sima de los Huesos crania (Sierra de Atapuerca, Spain). a comparative study. J. Hum. Evol. 33, 219–281.

Bastir, M., 2008. A systems-model for the morphological analysis of integration and modularity in human craniofacial evolution. J. Anthropol. Sci. 86, 37–58.

Bastir, M., Rosas, A., 2006. Correlated variation between the lateral basicranium and the face: a geometric morphometric study in different human groups. Arch. Or. Biol. 51, 814–824.

Bastir, M., O'Higgins, P., Rosas, A., 2007. Facial ontogeny in Neandertals and modern humans. Proc. R. Soc. Lond. B 274, 1125–1132.

Bastir, M., Rosas, A., Kuroe, K., 2004. Petrosal orientation and mandibular ramus breadth: evidence of a developmental integrated petroso-mandibular unit. Am. J. Phys. Anthropol. 123, 340–350.

Bastir, M., Rosas, A., Lieberman, D.E., O'Higgins, P., 2008. Middle cranial fossa anatomy and the origins of modern humans. Anat. Rec. 291, 130–140.

Bookstein, F.L., 1991. Morphometric Tools for Landmark Data. Cambridge University Press, Cambridge.

Caspari, R., 2005. The suprainiac fossa: the question of homology. Anthropol. 43, 229–239.

Caspari, R., 2006. The Krapina occipital bones. Period. Biolog. 108, 299–307.

Caspari, R., Radovcić, J., 2006. New reconstruction of Krapina 5, a male Neandertal cranial vault from Krapina, Croatia. Am. J. Phys. Anthropol. 130, 294–307.

Churchill, S.E., Smith, F.H., 2000. Makers of the early Aurignacian of Europe. Yrbk. Phys. Anthropol. 43, 61–115.

Condemi, S., 2001. Les Néandertaliens de La Chaise Éd. du CTHS, Paris.

Dean, D., Hublin, J.-J., Holloway, R., Ziegler, R., 1998. On the phylogenetic position of the pre-Neandertal specimen from Reilingen, Germany. J. Hum. Evol. 34, 485–508.

Enlow, D.H., 1990. Facial Growth. W.B. Saunders Company, Philadelphia.

Feneis, H., 1982. Anatomisches Bildwörterbuch. Georg Thieme Verlag, Stuttgart.

Fortea, J., de la Rasilla, M., Martínez, E., Sánchez-Moral, S., Cañaveras, J.C., Cuezva, S., Rosas, A., Soler, V., Juliá, R., Torres, T., Ortiz, J.E., Castro, J., Badal, E., Altuna, J., Alonso, J., 2003. La cueva de El Sidrón (Borines, Piloña, Asturias): Primeros resultados. Estud. Geol. 59, 159–179.

Frayer, D., Wolpoff, M., 1985. Sexual dimorphism. Ann. Rev. Anthrop. 14, 429–473.

Gunz, P., Harvati, K., 2007. The Neandertal "chignon": variation, integration, and homology. J. Hum. Evol. 53, 732–746.

Gunz, P., Mitteroecker, P., Bookstein, F.L., Weber, G., 2004. Computer aided reconstruction of incomplete human crania using statistical and geometrical estimation methodsEnter the Past: Computer Applications and Quantitative Methods in Archaeology. BAR Intl. Ser. 1227, 92–94. Archaeopress:Vienna.

Harvati, K., 2001. The Neanderthal problem: 3-D geometric morphometric models of cranial shape variation within and among species. Ph. D. Dissertation, City University of New York.

Hublin, J.-J., 1978. Le Torus Occipital Transverse et les Structures Associées: Évolution dans le Genre *Homo*. PhD Dissertation, Paris VI University, Paris.

Hublin, J.-J., 1984. The fossil man from Salzgitter-Lebenstedt. Z. Morph. Anthrop. 75, 45–56.

Hublin, J., 1998. Climatic changes, paleogeography, and the evolution of the Neandertals. In: Akazawa, T., Aoki, K., Bar-Yosef, O. (Eds.), Neandertals and Modern Humans in Western Asia. Plenum Press, New York, pp. 295–310.

Mardia, K.V., Bookstein, F.L., Moreton, I.J., 2000. Statistical assessment of bilateral symmetry of shapes. Biometrika 87, 285–300.

O'Higgins, P., 2000. The study of morphological variation in the hominid fossil record: biology, landmarks and geometry. J. Anat. 197, 103–120.

Rehg, J.A., Leigh, S.R., 1999. Estimating sexual dimorphism and size differences in the fossil record: a test of methods. Am. J. Phys. Anthropol. 110, 95–104.

Rightmire, G., 2004. Brain size and encephalization in early to Mid-Pleistocene *Homo*. Am. J. Phys. Anthropol. 124, 109–123.

Rohlf, F., 1997. NTSYS-pc: Numerical Taxonomy and Multivariate Analysis System. Exeter Software, Setauket, New York.

Rohlf, F.J., Slice, D., 1990. Extensions of the procrustes method for the optimal superimposition of landmarks. Syst. Zool. 39, 40–59.

Rosas, A., Aguirre, E., 1999. Restos humanos Neandertales de la cueva del Sidrón, Piloña, Asturias: nota preliminar. Estud. Geol. 55, 181–190.

Rosas, A., Bastir, M., 2002. Thin-plate spline analysis of allometry and sexual dimorphism in the human craniofacial complex. Am. J. Phys. Anthropol. 117, 236–245.

Rosas, A., Bermúdez de Castro, J.M., 1998. The mauer mandible and the evolutionary significance of *Homo heidelbergensis*. Geobios 31, 687–697.

Rosas, A., Bastir, M., Martínez Maza, C., Bermúdez de Castro, J.M., 2002. Sexual dimorphism in the Atapuerca-SH hominids: the evidence from the mandibles. J. Hum. Evol. 42, 451–474.

Rosas, A., Martínez-Maza, C., Bastir, M., García-Tabernero, A., Lalueza-Fox, C., Huguet, R., Estalrrich, A., García-Vargas, S., de la Rasilla, M., Fortea, J., 2007. Paleobiological aspects of El Sidrón (Asturias, Spain) Neandertals. Am. J. Phys. Anthropol. S44, 202.

Rosas, A., Martínez-Maza, C., Bastir, M., Garcia-Tabernero, A., Lalueza-Fox, C., Huguet, R., Ortiz, J.E., Julia, R., Soler, V., Torres, T.D., Martínez, E., Cañaveras, J.C., Sanchez-Moral, S., Cuezva, S., Lariol, J., Santamaria, D., de la Rasilla, M., Fortea, J., 2006. Paleobiology and comparative morphology of a late Neandertal sample from El Sidrón, Asturias, Spain. Proc. Natl. Acad. Sci. 103, 19266–19271.

Rosas, A., Peña, A., Garcia-Tabernero, A., Bastir, M., De la Rasilla, M., Fortea, J., 2008. Endocranial occipito-temporal anatomy of the SD-1219 fossil from the El Sidrón Neandertals. Anat. Rec. 291, 502–512.

Ruff, C.B., Trinkaus, E., Holliday, T.W., 1997. Body mass and encephalization in Pleistocene *Homo*. Nature 387, 173–176.

Santa Luca, A.P., 1978. A re-examination of presumed Neandertal-like fossils. J. Hum. Evol. 31, 21–39.

Sládek, V., 2000. Hominid Evolution in Central EUROPE during Upper Pleistocene: Origin of Anatomically Modern Humans. University of Bordeaux 1, Bordeaux.

Smith, F., 1980. Sexual differences in European Neandertal crania with special reference to the Krapina crania. J. Hum. Evol. 9, 359–375.

Smith, F., Trinkaus, E., 1991. Les origines de l'homme moderne en Europe centrale: un cas de continuité. In: Hublin, J.-J., Tillier, A.M. (Eds.), Aux origines d'*Homo sapiens* Nouvelle Encyclopédie. Diderot, pp. 251–290.

Spitery, E., 1985. Principaux caractères évolutifs de l'os occipital chez les hominides fossiles. L'Anthropologie 89, 75–91.

StatSoft, I., 1999. STATISTICA for Windows. StatSoft, Tulsa, OK.

Tattersall, I., Sawyer, G.J., 1996. The skull of "*Sinanthropus*" from Zhoukoudian, China: a new reconstruction. J. Hum. Evol. 31, 311–314.

Torres, T., Ortíz, J.E., Grün, R., Eggins, S., Valladas, H., Mercier, N., Tisnérant-Laborde, N., Juliá, R., Soler, V., Martínez, E., Cañaveras, J.C., Sánchez Moral, S., Lario, J., Badal, E., Lalueza-Fox, C., Rosas, A., Santamaría, M., De la Rasilla, M., Fortea, J. Dating of the hominid (*Homo neanderthalensis*) remains accumulation from El Sidrón Cave (Piloña, Asturias, North Spain): an example of multi-methodological approach to the dating of Upper Pleistocene sites. Geoarchaeol, in press.

Trinkaus, E., LeMay, M., 1982. Occipital bunning among later Pleistocene hominids. Am. J. Phys. Anthropol. 57, 27–35.

von Cramon-Taubadel, N., 2009. Congruence of individual cranial bone morphology and neutral molecular affinity patterns in modern humans. Am. J. Phys. Anthropol. 140, 205–215.

Wiley, D.F., Amenta, N., Alcantara, D.A., Ghosh, D., Kil, Y.J., Delson, E., Harcourt-Smith, W., Rohlf, F.J., St. John, K., Hamann, B., 2005. Evolutionary morphing. VIS 05. IEEE, 431–438.